Supplemental Material:

Bacterial cell wall biogenesis is mediated by SEDS and PBP polymerase families functioning semi-autonomously

Hongbaek Cho[1]*, Carl N. Wivagg[2]*, Mrinal Kapoor[2]*, Zachary Barry[2], Patricia D.A. Rohs[1], Hyunsuk Suh[3], Jarrod A. Marto[3,4], Ethan C. Garner[2]**, Thomas G. Bernhardt[1]**

*contributed equally
**corresponding authors

[1]Department of Microbiology and Immunobiology
Harvard Medical School
Boston, MA 02115

[2]Department of Molecular and Cellular Biology
Harvard University
Cambridge, Massachusetts 02138

[3]Department of Biological Chemistry and Molecular Pharmacology
Harvard Medical School
Boston, MA 02115

[4]Department of Cancer Biology and Blais Proteomics Center
Dana-Farber Cancer Institute
Boston, MA 02215

**To whom correspondence should be addressed.

Thomas G. Bernhardt, Ph.D.
Harvard Medical School
Department of Microbiology and Immunobiology
Boston, Massachusetts 02115
e-mail: thomas_bernhardt@hms.harvard.edu

Ethan C. Garner
Harvard University
Department of Molecular and Cellular Biology
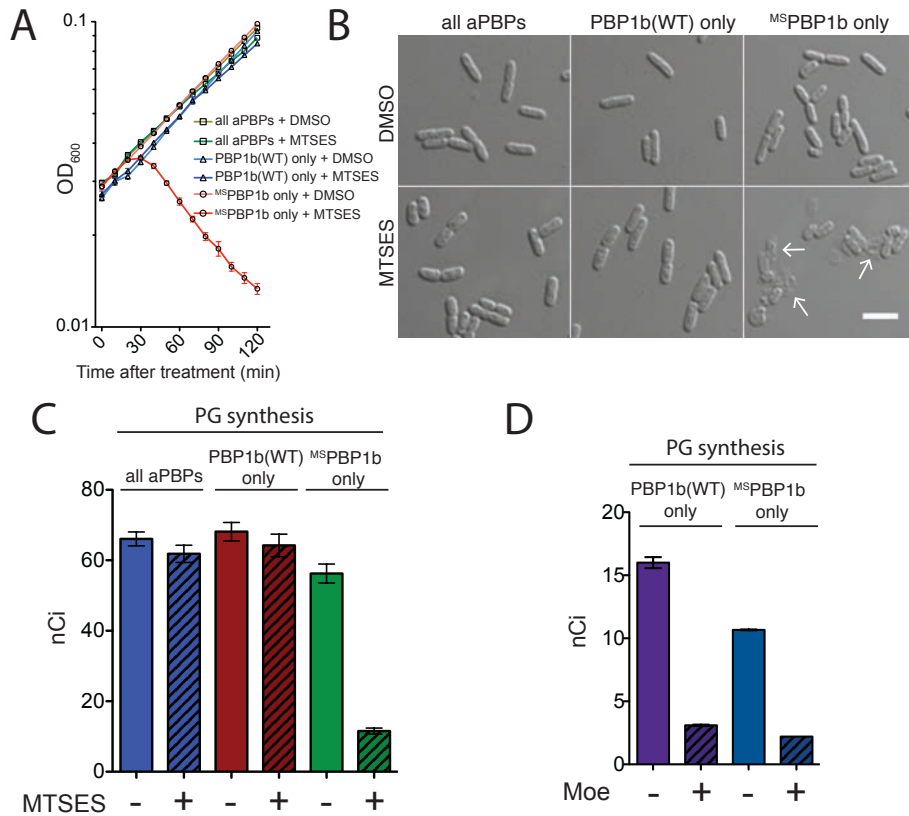Cambridge, Massachusetts 02138
e-mail: egarner@fas.harvard.edu

Figure S1. Functionality of ^{MS}PBP1b and specificity of inhibition with MTSES.
A. MTSES-sensitive growth is only observed for cells containing ^{MS}PBP1b as their sole aPBP. Cells of MG1655 [WT] (labeled all aPBPs), HC545 [ΔponA ΔpbpC ΔmtgA ponB(WT)] (labeled PBP1b(WT) only), and HC546 [ΔponA ΔpbpC ΔmtgA ^{MS}ponB] (labeled ^{MS}PBP1b only) were grown overnight in M9-glucose supplemented with 0.2% casamino acids at 37°C. The resulting cultures were diluted 1:100 in the same medium and grown at 37°C to exponential phase. The OD_{600} of each culture was adjusted to 0.1 with fresh medium and DMSO (control) or MTSES (1mM) were added as indicated. A small volume of each culture (150 µl) was then transferred to Corning 96-well plates (ref. 3598) and OD_{600} was monitored during growth with shaking at 37°C in a VersaMax microplate reader (Molecular Devices). Note, OD_{600} values from the plate reader are lower than those measured from cultures due to a difference in path length. **B. Effect of MTSES on cell morphology.** Cells prepared from cultures grown similarly to those in (A) were harvested and fixed 45 min after treatment with DMSO (control) or MTSES (1mM). Fixed cells were then imaged on agarose pads using DIC optics. Scale bar equals 4 microns. Arrows point to lysed cells. **C. Specificity of PG synthesis inhibition by MTSES.** Overnight cultures of HC516 [ΔlysA ΔampD] (labeled all aPBPs), HC526 [ΔlysA ΔampD ΔponA ΔpbpC ΔmtgA ponB(WT)] (labeled PBP1b(WT) only), and HC533 [ΔlysA ΔampD ΔponA ΔpbpC ΔmtgA ^{MS}ponB] (labeled ^{MS}PBP1b only) all harboring an integrated P_{tac}::sulA construct (attλHC739) were diluted to OD_{600} = 0.04 in fresh M9-glycerol medium supplemented with 0.2% casamino acids. Cultures were then grown at 30°C to OD_{600} between 0.27-0.30, at which time IPTG (1 mM) was added to induce sulA expression. After 30 minutes of additional growth and an adjustment of each culture to an OD_{600} of 0.3, MTSES (1 mM) or an equivalent amount of DMSO was added. Following 5 additional minutes of growth, 0.5 ml of each culture was incubated with 1 µCi [³H]-mDAP for 10 min at 30°C before mDAP incorporation was stopped by boiling the samples for 30 min at 90°C. The boiled samples were pelleted, washed, and digested with 250 µg HEW lysozyme overnight at 37°C. The radioactivity released by lysozyme treatment was quantified by scintillation counting. **D. PG synthesis is inhibited by moenomycin to a similar degree as MTSES-treatment of ^{MS}PBP1b-containing cells.** Cells of HC590 [imp4213 ΔlysA ΔponA ΔpbpC ΔmtgA ponB(WT)] (labeled PBP1b(WT) only), and HC591 [imp4213 ΔlysA ΔponA ΔpbpC ΔmtgA ^{MS}ponB] (labeled ^{MS}PBP1b only) harboring an integrated P_{tac}::sulA construct (attλHC739) were grown and labeled with [³H]-mDAP as above. However, in place of MTSES, cells were treated with 10 µg/mL moenomycin (Moe). Note that the strains used here are outer membrane compromised (imp4213) derivatives of the strains in (C) to allow for moenomycin entry. Microscopy and growth data are representative of at least two independent experiments. Radiolabeling results are the average of three independent experiments with the error bars representing the standard error of the mean.
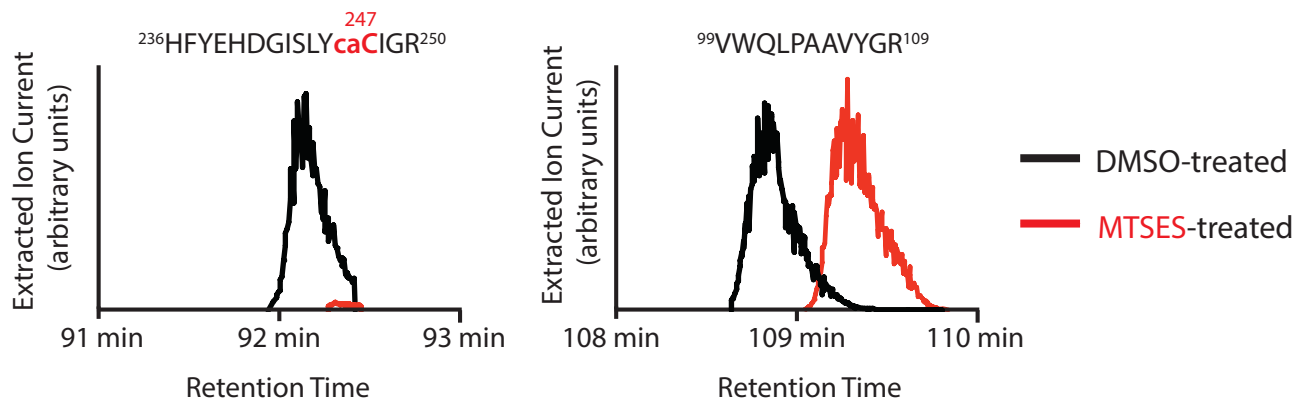
Figure S2. Mass Spectrometry analysis of MSPBP1b modification by MTSES. Shown are extracted ion current (XIC) chromatograms for the indicated tryptic peptides of MSPBP1b prepared from cells with or without MTSES treatment. The Cys247-containing peptide (left, z = +3 species) was only detected in the mock (DMSO) treated sample, indicating virtually complete modification by MTSES. However, equivalent levels of the peptide from residue 99-109 (right) were detected regardless of treatment. Note, **caC** indicates carbamidomethylated cysteine generated by iodoacetamide treatment used to protect Cys-containing peptides during sample preparation. Also see Table S1. Results are from a single experiment with multiple samples.
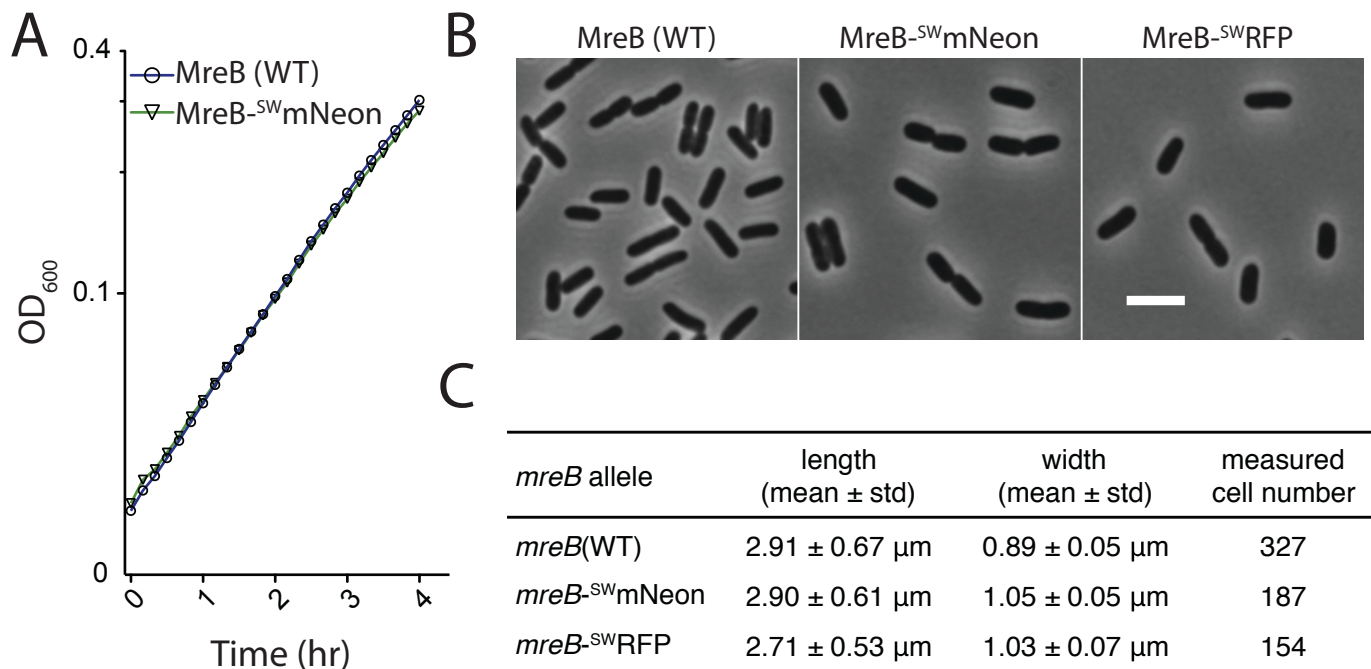
A.

OD$_{600}$ vs Time (hr)

- MreB (WT)
- MreB-^{SW}mNeon

B. MreB (WT) | MreB-^{SW}mNeon | MreB-^{SW}RFP

C.

mreB allele	length (mean ± std)	width (mean ± std)	measured cell number
mreB(WT)	2.91 ± 0.67 μm	0.89 ± 0.05 μm	327
mreB-^{SW}mNeon	2.90 ± 0.61 μm	1.05 ± 0.05 μm	187
mreB-^{SW}RFP	2.71 ± 0.53 μm	1.03 ± 0.07 μm	154

Figure S3. Functionality of the MreB-^{SW}mNeon fusion.
A. Growth of MreB-^{SW}mNeon producing cells is normal. Cells of HC546 [Δ*ponA* Δ*pbpC* Δ*mtgA* ^{MS}*ponB*] and its derivative HC583 harboring *mreB*-^{SW}mNeon replacing *mreB* at the native locus, were grown and OD$_{600}$ was monitored as in Figure S1A. Results are representative of duplicate experiments.

B-C. Cell morphology is largely normal in MreB-^{SW}mNeon producing cells.
Overnight cultures of the strains in (A) as well as HC582, also a derivative of HC546, but with *mreB*-^{SW}RFP at the native *mre* locus, were diluted (1:100) in M9-glucose medium supplemented with 0.2% casamino acids and grown at 37°C to an OD$_{600}$ of 0.3. Cells were then imaged on agarose pads using phase contrast optics. Scale bar, 4 microns. Panel (C) shows length and width measurements of cells imaged as in (B). Measurements were made using Oufti (1). Results are representative of duplicate experiments.
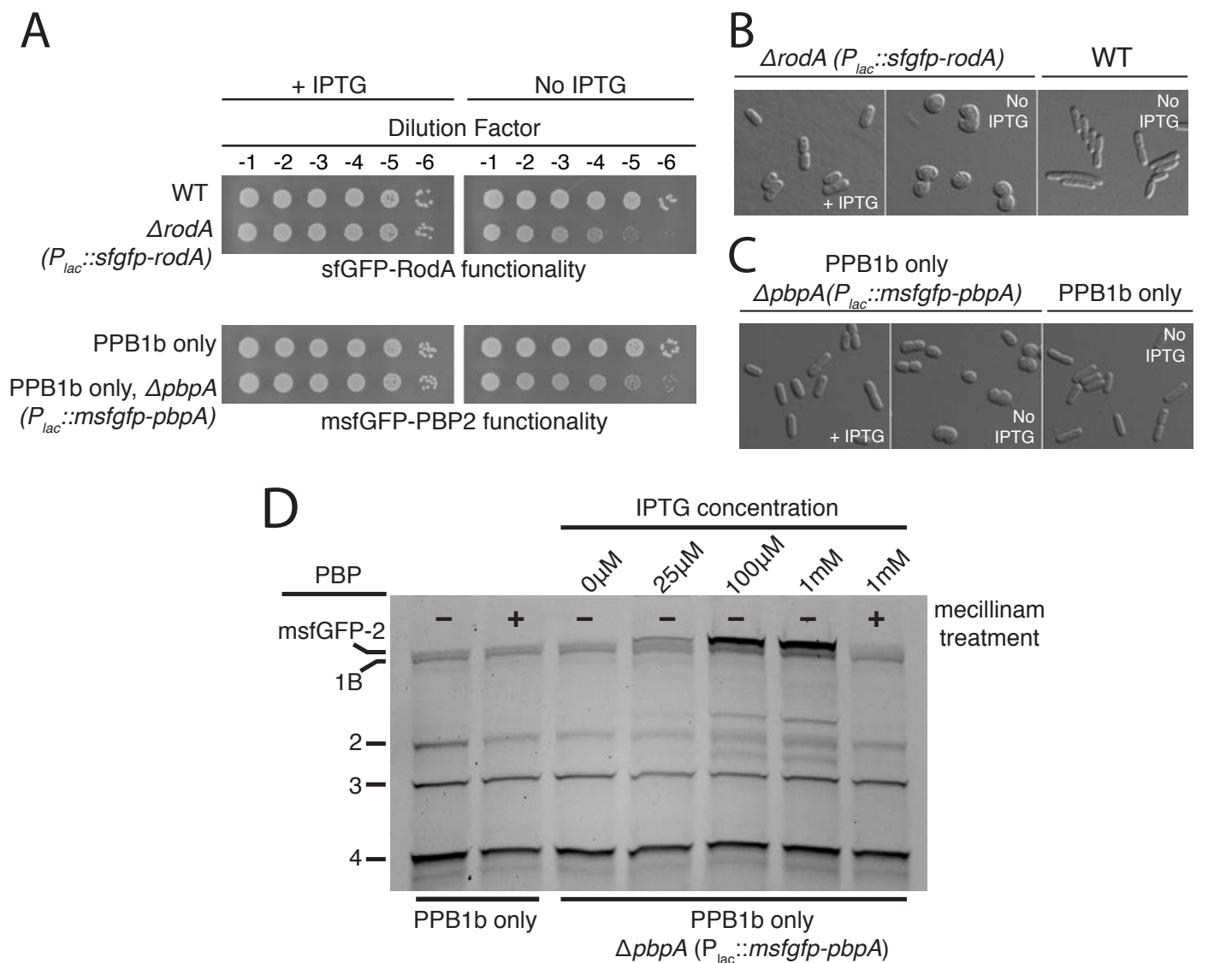
Figure S4. Functionality of PBP2 and RodA fluorescent protein fusions.
A. RodA or PBP2 fusion production corrects the growth phenotypes of *rodA* or *pbpA* deletion mutants, respectively. Overnight cultures of TB28 [WT], HC595(*att*HKpHC933) [Δ*rodA* (P$_{lac}$::*sfgfp-rodA*)], HC545 [Δ*ponA* Δ*pbpC* Δ*mtgA*] (labeled PBP1b only) or HC596(*att*HKHC943) [PBP1b only Δ*pbpA* (P$_{lac}$::*msfgfp-pbpA*)] were serially diluted and spotted on M9 minimal maltose agar for the RodA functionality test or M9 minimal glucose agar for the PBP2 functionality test. Media was additionally supplemented with 0.2% casamino acids as well as IPTG as indicated (100 μM for *sfgfp-rodA* or 25 μM *msfgfp-pbpA*).
B-C. Cell morphology of the fluorescent protein fusion strains grown with or without induction of fluorescent protein fusions. Overnight cultures of the strains in (A) grown in the presence of IPTG were washed with M9 minimal medium, diluted to an OD$_{600}$ of 0.001, and grown to exponential phase in M9 minimal medium with or without IPTG induction. Sugar, casamino acid, and IPTG supplementation were as in (A).
D. Measurement of relative msfGFP-PBP2 concentration by Bocillin binding. Overnight cultures of HC545 [Δ*ponA* Δ*pbpC* Δ*mtgA*] (labeled PBP1b only) or HC596(*att*HKHC943) [PBP1b only Δ*pbpA* (P$_{lac}$::*msfgfp-pbpA*)] were diluted and grown as in (B-C). Cells harvested from 15 ml of exponential cultures were labeled with Bocillin (see Methods). A subset of cultures were treated with 10 μg/mL mecillinam, which reacts with the TP active site of PBP2 and blocks Bocillin binding, 5 min prior to harvesting and labeling. All results are representative of at least duplicate experiments.
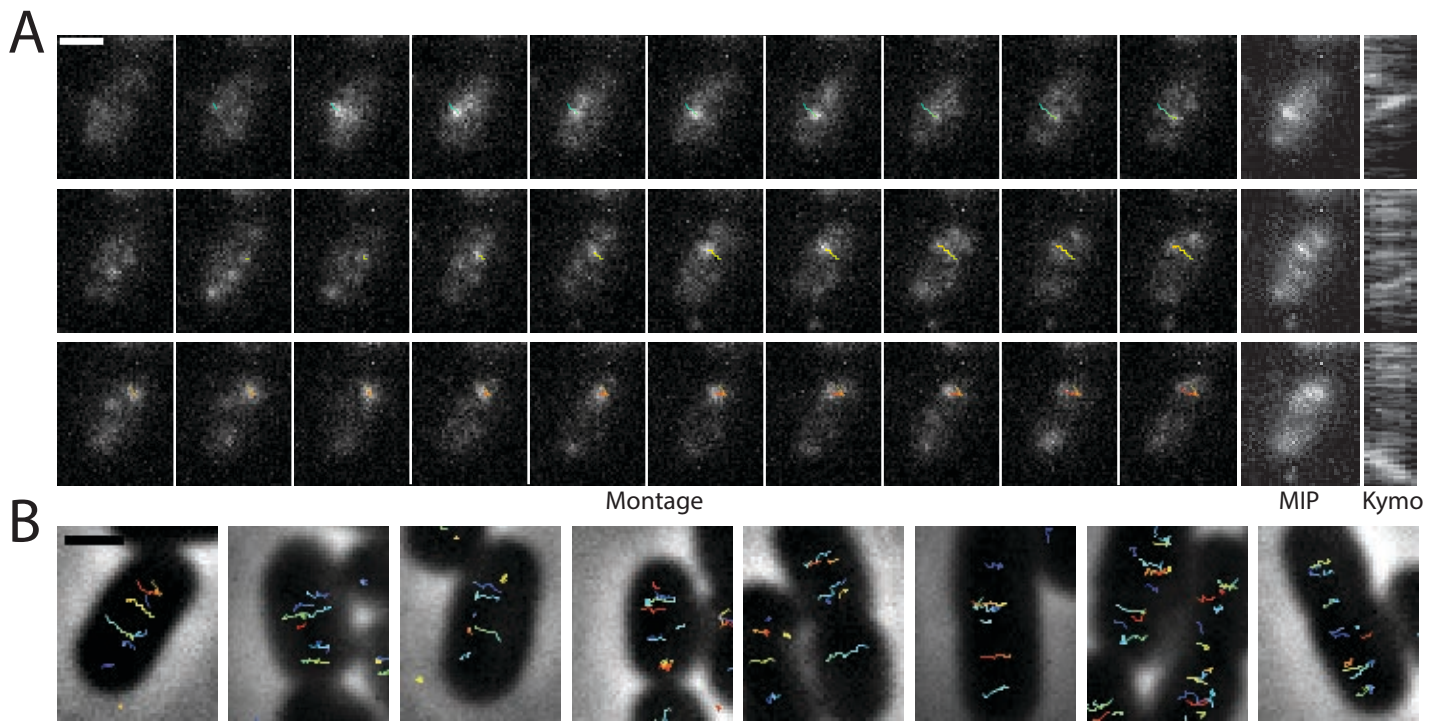
A

Montage   MIP Kymo

B

Figure S5. RodA moves circumferentially around the the cell cylinder. A. Montage of RodA movement in HC595(attHKpHC933) [Δ*rodA* (P$_{lac}$::*sfgfp-rodA*)] shows directional motion. Maximal intensity projection (MIP) and kymograph (Kymo) frames were collected every 1 s, montage frames every 2 s. Displayed are raw trajectories not filtered for speed or log log fits to α. **B.** Phase contrast images with track overlays show additional examples of RodA directional motion. Scale bars are 1 μm. Results are representative of two independent experiments.
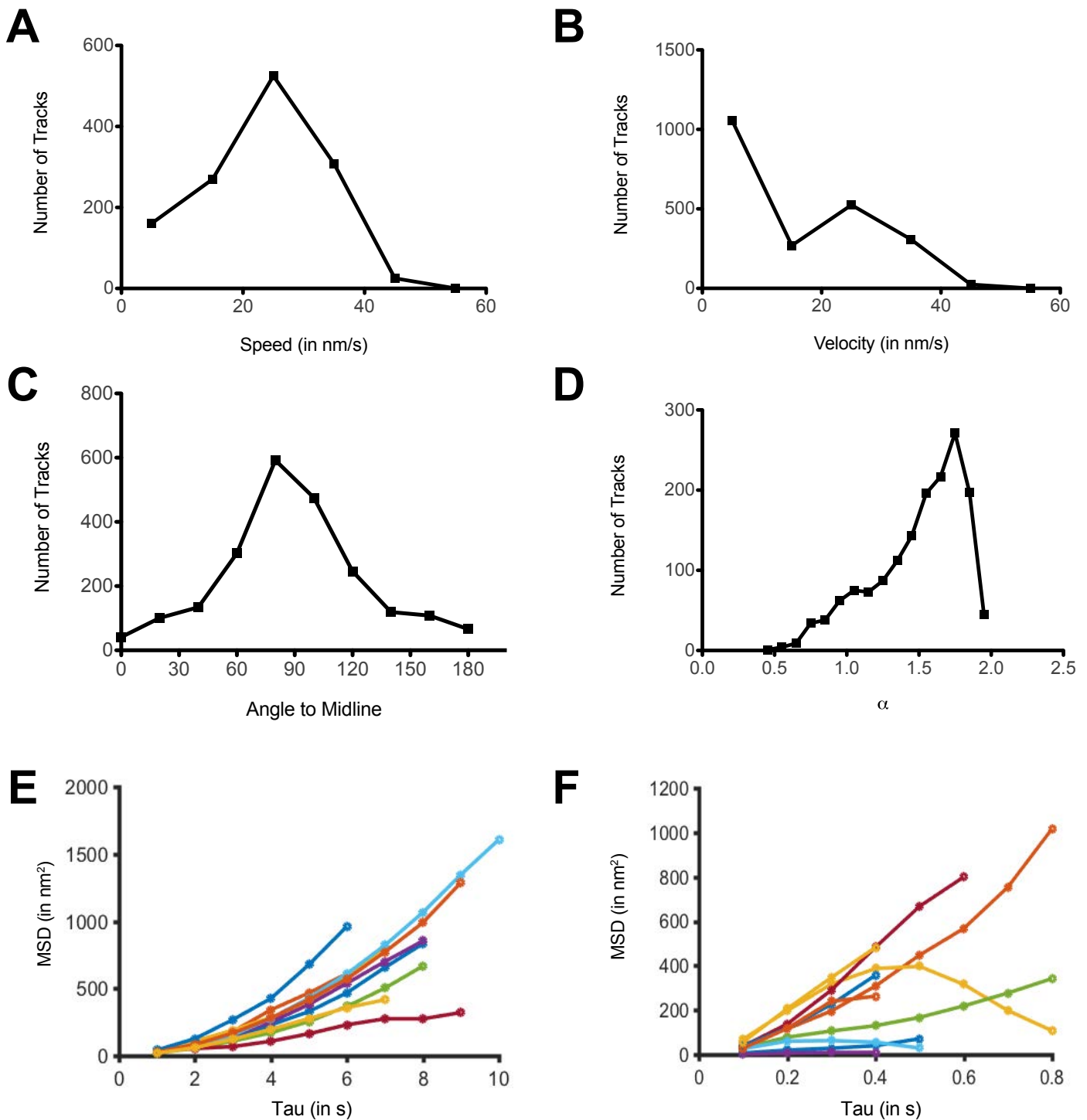
Figure S6. PBP2 moves circumferentially around the the cell cylinder. A. Histogram of directionally moving particles (velocity > 0.01 nm/s) without filtering by α fit as described in Materials and Methods. **B.** Histogram of all velocities, including non-directional particles (velocity <0.01 nm/s). **C.** Histogram of all angles to the cell midline without filtering on R^2 fits to a line. **D.** Histogram of the scaling exponent α (filtered for linear fits to the log-log of α and velocity >0.01 nm/s as described in Materials and Methods) with a median value of 1.65, indicating directed motion. **E.** MSD vs. τ for randomly selected individual PBP2 tracks. **F.** MSD vs. τ for randomly selected individual *B. subtilis* PBP1 tracks from strain MK210. Results are representative of two independent experiments.
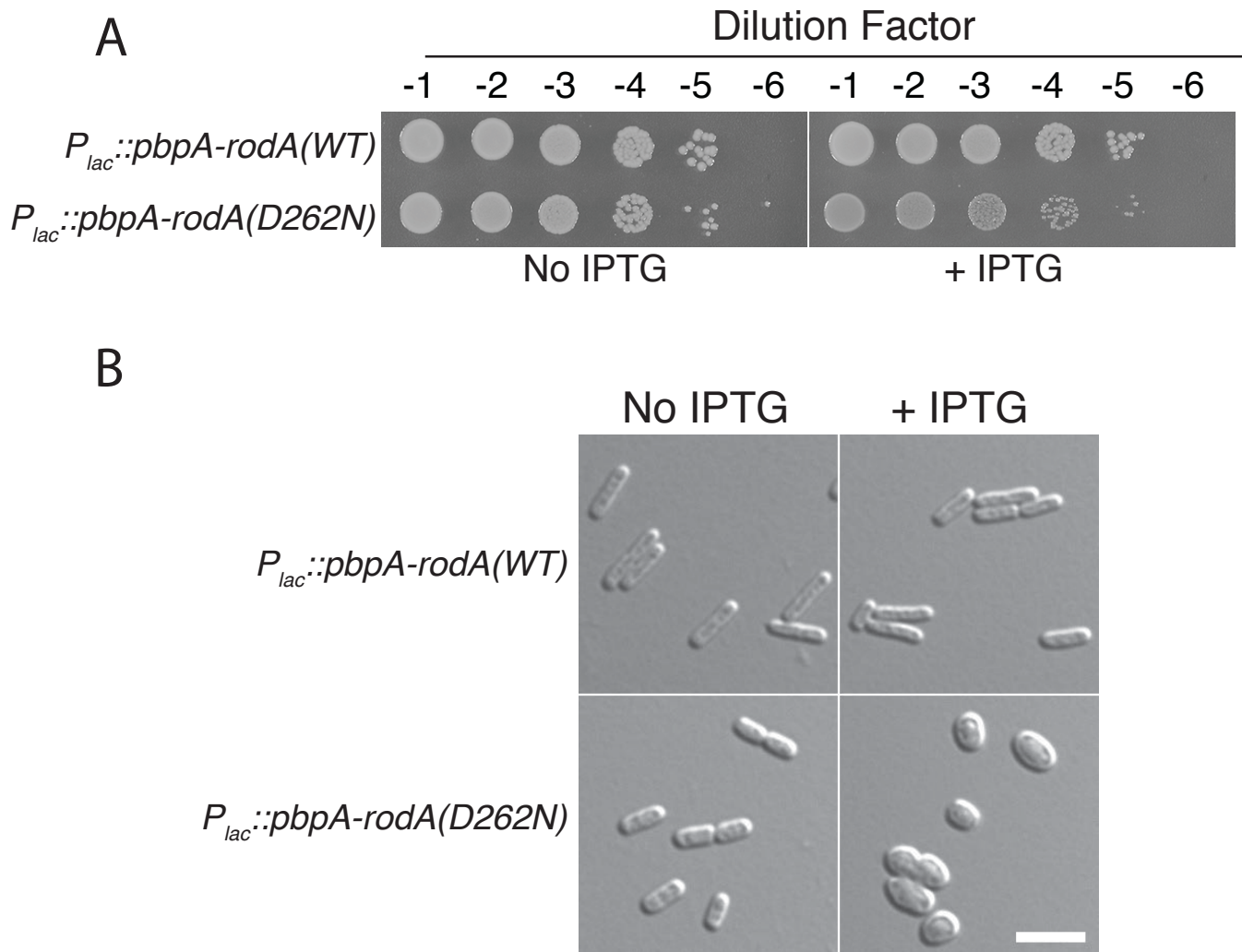
Figure S7. Dominant-negative activity of RodA(D262N).
A. Overexpression of RodA(D262N) causes a growth defect. Cells of TB28 [WT] harboring both an integrated $P_{tetA}::mreB$-$_{sw}mNeon$ construct (attHKHC929), and either pHC857 [$P_{lac}::pbpA$-$rodA(WT)$] or pHC938 [$P_{lac}::pbpA$-$rodA(D262N)$], were grown overnight at 37°C in M9-maltose supplemented with 0.2% casamino acids and 10 μg/mL chloramphenicol. Serial dilutions of these cultures were spotted onto agar plates of the same medium composition, with or without 1 mM IPTG.
B. Effect of RodA(D262N) overexpression on cell morphology. The cultures described in (A) were diluted to an OD_{600} of 0.05 and grown at 37°C until the OD_{600} reached between 0.2 and 0.3. These exponential-phase cultures were then further diluted (to an OD_{600} of 0.005) in the presence or absence of 1 mM IPTG. Cells were fixed when the OD_{600} reached between 0.1 and 0.15, then imaged on agarose pads using DIC optics. Scale bar, 4 microns. Results in both panels are representative of two independent experiments.
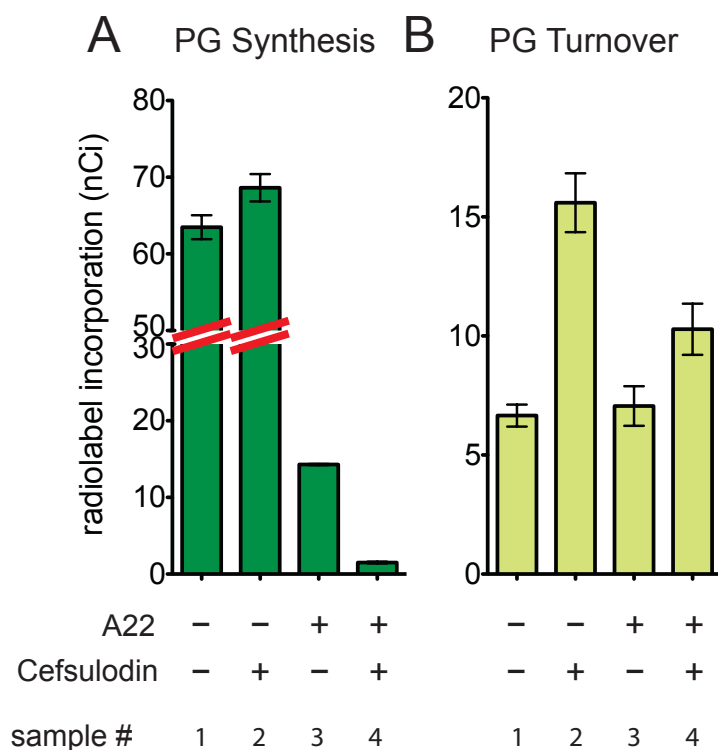
Figure S8. PBP1a polymerizes PG without a functional cytoskeleton.
A-B. PG matrix assembly and turnover were measured upon treatment of strain PR70(attHKHC739) [Δ*lysA* Δ*ampD* Δ*pbpC* Δ*mtgA* Δ*ponB* (P$_{tac}$::*sulA*)] with cefsulodin and/or A22. Measurements were made as described in Figure 2 and 4. Cefsulodin and A22 were used at 100 µg/ml and 10 µg/mL, respectively. Note that this strain produces PBP1a as its only aPBP. Significant PG synthesis activity is detected upon A22 treatment (sample 3), which inactivates MreB in cells already inactivated for FtsZ by SulA expression. This activity is converted to turnover by the PBP1a-specific beta-lactam cefsulodin (sample 4). We thus conclude that, like PBP1b, PBP1a remains active when all cytoskeletal elements are inactivated in *E. coli*. Results are the average of three independent experiments with the error bars representing the standard error of the mean.
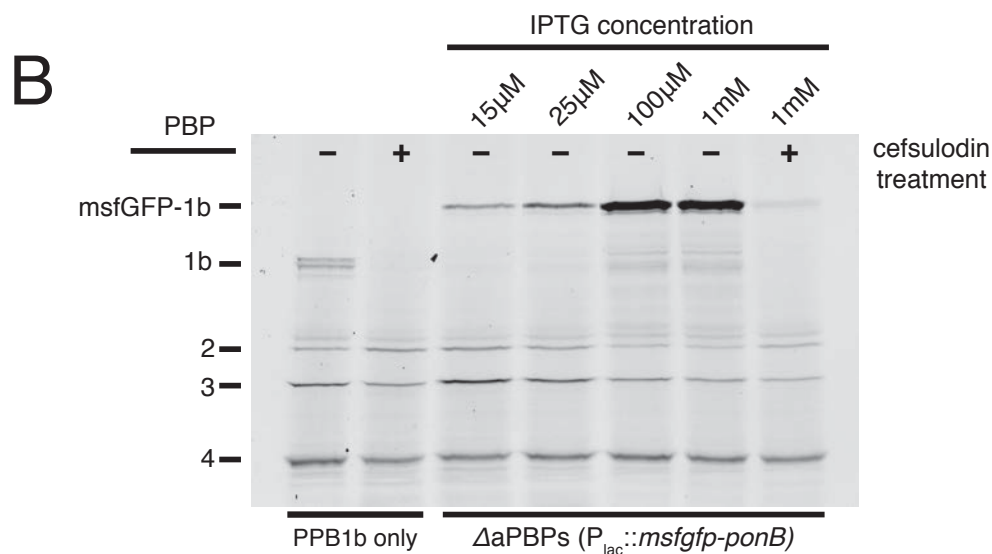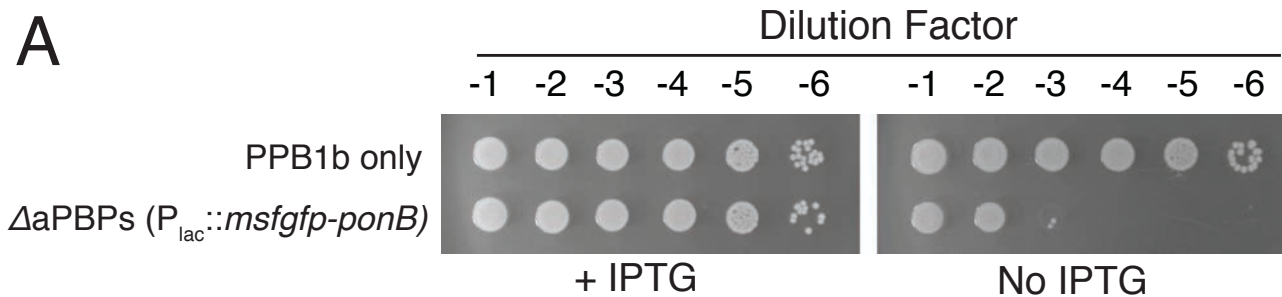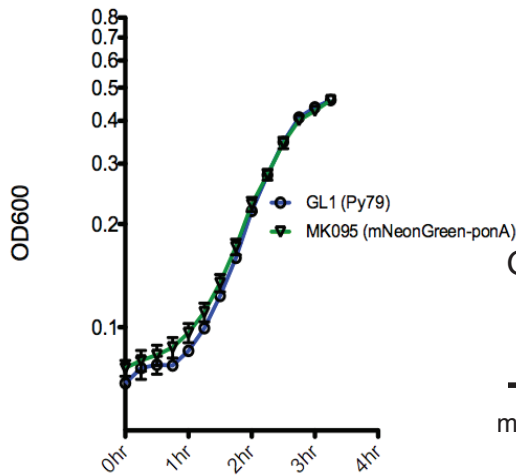
Figure S9. Functionality of msfGFP-PBP1b.
A. msfGFP-PBP1b supports growth as the sole aPBP. Cultures of HC545 [Δ*ponA* Δ*pbpC* Δ*mtgA*] (labeled PBP1b only) and HC576(attHKHC942)[Δ*ponA* Δ*pbpC* Δ*mtgA* Δ*ponB* (P$_{lac}$::*msfgfp-ponB*)] (labeled ΔaPBPs) were grown overnight in M9-glucose medium supplemented with 0.2% casamino acids with 25 *μ*M IPTG. Cell were then washed and serially diluted in the same medium lacking IPTG. Aliquots (5 *μ*L) of each dilution were then spotted on M9-glucose agar supplemented with 0.2% casamino acids with or without 25 *μ*M IPTG as indicated. The plates were incubated for 24 hrs at 37°C and imaged.
B. Measurement of relative msfGFP-PBP1b concentration by Bocillin binding. Cultures of the strains in (A) were diluted, grown, and labeled with Bocillin as in **Fig. S3D**. Indicated cultures were treated with 100 µg/mL cefsulodin for 5 min prior to harvesting and labeling. Note that the doublet band for PBP1b in lane one corresponds to the alpha and gamma forms of PBP1b produced from alternate start codons. The msfGFP-PBP1b fusion is to the shorter gamma form. Results in both panels are representative of at least two independent experiments.

Figure S10. Functionality of mNeon-PBP1 fusion in *B. subtilis*. A. Growth curves of Py79 [WT] and MK095 [*ponA::mNeonGreen-ponA*] strains. **B.** Cell width measurements of Py79 [WT], MK005 [Δ*ponA*], MK287 [Δ*ponA; amyE::Phyperspank-mNeonGreen-ponA*], and MK095 [*ponA::mNeonGreen- ponA*], strains. For MK287, mNeon-PBP1 was induced by addition of 10 *µ*M IPTG. **Measurement of relative mNeon-PBP1 concentration by Bocillin binding. C.** Overnight cultures of strains Py79, MK005, MK287, and MK095 (left to right) were diluted into fresh CH medium, grown for two hours at 37 °C, and labeled with Bocillin as in **Fig. S3D**. Note that the concentration of mNeon-PBP1 expressed from its native promoter (MK095, rightmost lane) is much less than that in wild-type (Py79, leftmost), explaining the failure of native *mNeonGreen-ponA* (*ponA::mNG-ponA*) to suppress the width phenotype of *ponA* deletion in MK095. Results are representative of two independent experiments.
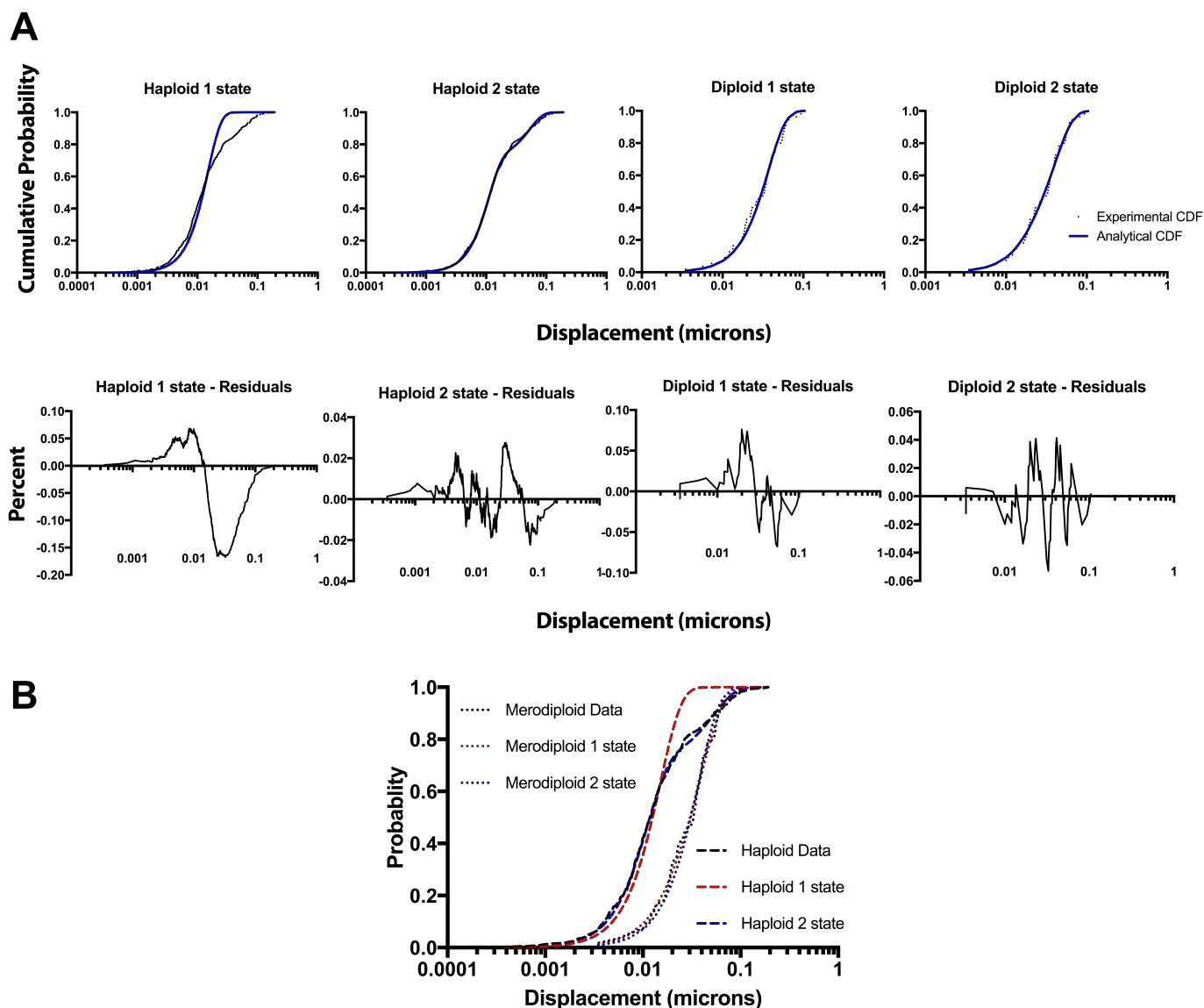
Figure S11. A. Cumulative distribution function (CDF) fitting of PBP1 displacements reveals two-state diffusive behavior. Top row: the analytical (blue) and experimental (black) CDF curves for haploid (MK287) and merodiploid (MK210) strain datasets. Bottom row: respective residuals for CDF model fits corresponding to the above CDF plots. The single-state haploid fitting has considerable residuals corresponding to the location of where a faster state of diffusion manifests, necessitating the introduction of a second state of diffusion for this enzyme into the CDF fitting. **B.** Comparison of the CDF model fits between merodiploid and haploid strains. The characteristic displacement magnitude of the two-state haploid strain CDF where the residuals hit the maximum value in the one-state model closely corresponds to that of the fast state of the merodiploid strain, suggesting both of these fast states may result from the same underlying biological phenomena. Microscopy data are representative of two independent experiments.

Original gel image for Figure S4D

Original gel image for Figure S9B
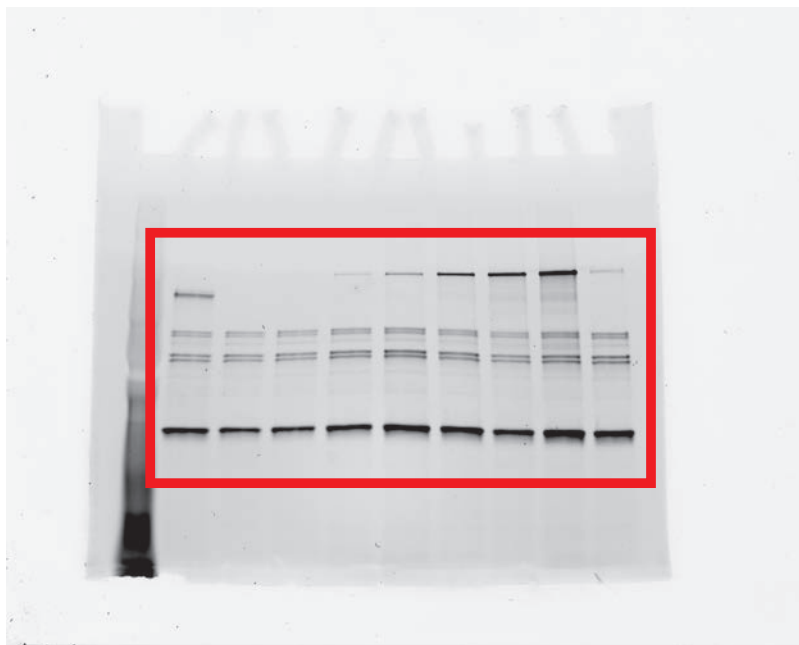
Original gel image for Figure S10C

Supplemental Video Legends

Supplemental Video S1. Inhibition of ^{MS}PBP1b does not affect MreB motion. Time-lapses of MreB-^{SW}mNeon were collected in HC546(attλHC897) [Δ*ponA* Δ*pbpC* Δ*mtgA* ^{MS}*ponB mreB*-^{SW}*mNeon*] at 0-15 min (early) following MTSES treatment and 30-45 (late) following MTSES treatment. Scale bar is 1 µm; time-lapses are continuous 1 s exposures under TIRF illumination.

Supplemental Video S2. RodA moves circumferentially around the cell axis in *E. coli*. Fluorescent microscopy images were collected in HC595(attHKHC933) [Δ*rodA* (P$_{lac}$::*sfgfp-rodA*)] by continuous acquisition with 1 s exposures. Colored tracks show the paths traversed by individual fluorescent particles. Scale bar is 1 µm; time-lapses are continuous 1 s exposures under TIRF illumination.

Supplemental Video S3. PBP2 moves circumferentially around the cell axis in *E. coli*. Fluorescent microscopy images were collected in HC596(attHKHC943) [Δ*ponA* Δ*pbpC* Δ*mtgA* Δ*pbpA* (P$_{lac}$::*msfgfp-pbpA*)] by continuous acquisition with 1 s exposures. Colored tracks show the paths traversed by individual fluorescent particles. Scale bar is 1 µm; time-lapses are continuous 1 s exposures under TIRF illumination.

Supplemental Video S4. PBP2 exhibits both diffusive and directional motion. Under constant induction in HC596(attHKHC943) [Δ*ponA* Δ*pbpC* Δ*mtgA* Δ*pbpA* (P$_{lac}$::*msfgfp-pbpA*)], different imaging conditions reveal different states of PBP2 motion: continuous acquisition with 100 ms exposures shows diffusive PBP2 motion, with slow-moving particles appearing as short-lived bright dots. At 1,000 ms exposures, diffusive particles are blurred and the remaining motion appears directional. Scale bar is 1 µm; exposures were performed under TIRF illumination.

Supplemental Video S5. Induction of RodA(D262N) inhibits MreB motion. Time-lapses of MreB-^{SW}mNeon were collected at 0-30, 150-180, and 210-240 min after induction of RodA(D262N) with 1 mM IPTG. Scale bar is 1 µm; time-lapses are continuous 1 s exposures under TIRF illumination.

Supplemental Video S6A. PBP1b exhibits fast diffusive motion in *E. coli*. Under constant induction in HC576(attHKHC942) [Δ*ponA* Δ*pbpC* Δ*mtgA* Δ*ponB* (P$_{lac}$::*msfgfp-ponB*)], different imaging conditions suggest rapid, diffusive PBP1b motion: continuous acquisition with 100 ms exposures shows many individually diffusing PBP1b particles with overlapping paths. At 1,000 ms exposures, diffusive particles form a blurred over many pixels, while some bright foci persist in one place for several frames, indicating states of transient mobility. In contrast to MreB, these particles are non-processive and do not persist for many frames. Scale bar is 1 µm. All imaging was performed with TIRF illumination.

Supplemental Video S6B. PBP1b exhibits fast diffusive motion in *E. coli*. Under constant 50 µM IPTG induction in HC576(attHKHC949) [Δ*ponA* Δ*pbpC* Δ*mtgA* Δ*ponB* (P$_{lac}$::*Halo-ponB*)], labelling with 6.25 nM JF549 [2] for 15 min and monitoring with 100 ms exposures shows individually diffusing PBP1b particles. Scale bar is 1 µm; exposures were performed under TIRF illumination.

Supplemental Video S7. PBP1a does not exhibit directional motion in *E. coli*. Under constant 25 µM IPTG induction in PR71(attHKPR104) [Δ*mgtA* Δ*ponA* Δ*pbpC* Δ*ponB::kan* (*Plac::msfGFP-ponA*)] different imaging conditions suggest rapid, diffusive PBP1a motion: continuous acquisition with 100 ms exposures shows many individually diffusing PBP1a particles with overlapping paths. At 1,000 ms exposures, diffusive particles form a blurred, shifting background, while some bright foci persist for several frames, indicating one or more stopped particles; in contrast to MreB, these particles are non-processive and do not persist for many frames. Scale bar is 1 µm; exposures were performed under TIRF illumination.

Supplemental Video S8. *B. subtilis* mNeon-PBP1 does not exhibit MreB-like motion. Time-lapses of MK095 [*ponA::mNeonGreen-ponA*], in which mNeon-PBP1 expressed from the native promoter is the sole source of PBP1, show two states of apparently diffusive PBP1 motion only. Continuous acquisition with TIRF illumination with 1,000 ms (first series of movies) and 300 ms (second series of movies) exposures shows some stationary PBP1 particles while other, more rapidly diffusing particles blur together. Scale bar = 1 µm.

Supplemental Video S9. *B. subtilis* mNeon-PBP1 is predominantly in the slower diffusive state at low induction levels. In MK287 [Δ*ponA; amyE::P$_{hyperspank}$-mNeonGreen-ponA*], in which mNeon-PBP1 is the sole source of PBP1, leaky expression from the P$_{hyperspank}$ promoter produces a density of fluorescent molecules ideal for particle tracking. Continuous acquisition with TIRF illumination and 100 ms exposures shows a preponderance of stationary PBP1 particles and some rapidly diffusing particles. Scale bar = 1 µm.

Supplemental Video S10. The slower diffusive state of *B. subtilis* mNeon-PBP1 is saturable. In MK210 [*amyE::P$_{hyperspank}$-mNeonGreen-ponA*], the native *ponA* locus is left intact. Leaky expression of mNeon-PBP1 from the P$_{hyperspank}$ promoter in the background of wild type PBP1 molecules shifts the balance between the two states of motion compared to MK287, where the only PBP1 in the cell is fluorescently labeled. Continuous acquisition with 100 ms exposures shows that the majority of molecules are now in the more rapidly diffusive state, with a minority of stationary molecules still present. Scale bar = 1 µm.

Table S1. Mass spectrometry analysis of MS-PBP1b modification by MTSES.

peptide sequence[1]	mono-isotopic mass	m/z (charge)	peak integration (DMSO)[2]	peak integration (MTSES)[2]	signal intensity ratio (MTSES/DMSO)
HFYEHDGISLYca**C**IGR[3]	1865.8519	933.9332 (+2)	1.03E+09	n.d.[8]	0
HFYEHDGISLYca**C**IGR[3]	1865.8519	622.9579 (+3)	4.76E+09	4.04E+07	0.008
HFYEHDGISLYca**C**IGR[3]	1865.8519	467.4703 (+4)	1.27E+09	n.d.[8]	0
HFYEHDGISLYse**C**IGR[3]	1948.79	975.4026 (+2)	n.d.[8]	1.56E+09	-
HFYEHDGISLYse**C**IGR[3]	1948.79	650.6042 (+3)	n.d.[8]	2.76E+09	-
VWQLPAAVYGR[4]	1258.6822	630.3484 (+2)	1.71E+10	1.71E+10	1.00
LLEATQYR[5]	992.5291	497.2718 (+2)	4.59E+07	4.21E+07	0.919
QFGFFR[6]	800.387	401.2058 (+2)	2.03E+10	1.76E+10	0.866
DSDGVAGWIK[7]	1046.5033	524.2589 (+2)	7.58E+08	7.93E+08	1.05

[1] ca**C** stands for carbamidomethylated cysteine generated by iodoacetamide treatment used to protect Cys-containing peptides during sample preparation. se**C** stands for sulfonatoethyl sulphide-linked cysteine generated by MTSES treatment.

[2] Signals corresponding to the peptides of the indicated m/z were integrated from the extracted ion chromatograms of DMSO-treated and MTSES-treated samples, respectively. The identity of each peak was further confirmed by tandem mass spectra.

[3] Peptide corresponding to PBP1b amino acids 236-250. Contains S247C substitution.

[4] Peptide corresponding to PBP1b amino acids 99-109.

[5] Peptide corresponding to PBP1b amino acids 127-134.

[6] Peptide corresponding to PBP1b amino acids 191-196.

[7] Peptide corresponding to PBP1b amino acids 829-838.

[8] not detected

Table S2. Bacterial strains used in this study.

Strain	Genotype[a]	Source/Reference[b]
E.coli strains		
MG1655	*rph ilvG rfb*-50	(Guyer et al., 1981)
TB10	*rph1 ilvG rfb-50 λΔcro-bio nad::Tn10*	(Johnson et al, 2004)
TB28	MG1655 Δ*lacIZYA*::*frt*	(Bernhardt and de Boer, 2004)
MC4100	*F- araD139 Δ(argF-lac)169 rpsL150 relA1 flB5301 deoC1 pstF25 rbsR*	Lab Stock
TU116	MG1655 Δ*lacIZYA*::*frt* Δ*ponB::aph*	(Paradis-Bleau et al, 2010)
HC439/pHC817	MG1655 Δ*pbpA::aph* / P$_{lac}$::*pbpA*	(Cho et al, 2014)
HC534(attHKCS8)	TB10 Δ*rodA::aph* (P$_{lac}$::*rodA*)	This Study
HC516	MG1655 Δ*lysA*::*frt* Δ*ampD*::*frt*	This Study
HC518	MG1655 Δ*lysA*::*frt* Δ*ponA*::*frt* aph-P$_{ara}$::*ponB*	This Study
HC523	MG1655 Δ*lysA*::*frt* Δ*ponA*::*frt* Δ*pbpC*::*frt* Δ*mtgA*::*frt*	This Study
HC526	MG1655 Δ*lysA*::*frt* Δ*ponA*::*frt* Δ*pbpC*::*frt* Δ*mtgA*::*frt* Δ*ampD*::*frt*	This Study
HC532	MG1655 Δ*lysA*::*frt* Δ*ponA*::*frt* Δ*pbpC*::*frt* Δ*mtgA*::*frt* *ponB(S247C)*	This Study
HC533	MG1655 Δ*lysA*::*frt* Δ*ponA*::*frt* Δ*pbpC*::*frt* Δ*mtgA*::*frt* *ponB(S247C)* Δ*ampD*::*frt*	This Study
HC545	MG1655 Δ*ponA*::*frt* Δ*pbpC*::*frt* Δ*mtgA*::*frt*	This Study
HC546	MG1655 Δ*ponA*::*frt* Δ*pbpC*::*frt* Δ*mtgA*::*frt* *ponB(S247C)*	This Study
CH138/pCX16	TB28 Δ*galK* [λc1857 (*cro-bioA*)::TetAR] *mreB*::P$_{EM7}$-*galK* Δ*yhdE::cat* / P$_{aadA}$::*sdiA*	gift from de Boer lab
HC582	HC546 *mreB'-mCherry-'mreB* Δ*yhdE::cat*	This Study
HC583	HC546 *mreB'-mNeonGreen-'mreB* Δ*yhdE::cat*	This Study
JAB027	MC4100 *imp4213 bamA6*	This Study
HC590	MG1655 Δ*lysA*::*frt* Δ*ponA*::*frt* Δ*pbpC*::*frt* Δ*mtgA*::*frt* *imp4213*	P1(JAB027) X HC523-*leu::Tn10*

Strain	Genotype[a]	Source/Reference[b]
HC591	MG1655 Δ*lysA*::*frt* Δ*ponA*::*frt* Δ*pbpC*::*frt* Δ*mtgA*::*frt* *ponB(S247C) imp4213*	P1(JAB027) X HC532-*leu*::*Tn10*
HC595(attHKHC933)	TB28 Δ*rodA::aph* (P$_{lac}$::*sfgfp-rodA*)	P1(HC534) X TB28(attHKHC933)
HC596(attHKHC943)	HC545 Δ*pbpA::aph* (P$_{lac}$::*msfgfp-pbpA*)	P1(HC439) X HC545(attHKHC943)
HC576(attHKHC942)	HC545 Δ*ponB::aph* (P$_{lac}$::*msfgfp-ponB*)	P1(TU116) X HC545(attHKHC942)
HC576(attHKHC949)	HC545 Δ*ponB::aph* (P$_{lac}$::*Halo-ponB*)	P1(TU116) X HC545(attHKHC949)
PR71(attHKPR104)	HC545 Δ*ponB::aph* (P$_{lac}$::*msfgfp-ponA*)	P1(TU116) X HC545(attHKPR104)
PR70	MG1655 Δ*lysA*::*frt* Δ*pbpC*::*frt* Δ*mtgA*::*frt* Δ*ampD*::*frt* Δ*ponB::aph*	This Study
HC527	MG1655 Δ*lysA*::*frt* Δ*pbpC*::*frt* Δ*mtgA*::*frt* Δ*ampD*::*frt*	This Study
B.subitilis strains		
PY79	WT	Garner lab stock
MK005	PY79 Δ*ponA*	This Study
MK095	PY79 *ponA::mNeonGreen-ponA*	This Study
MK210	PY79 *amyE*::P$_{hyperspank}$-*mNeonGreen-ponA*	This Study
MK287	PY79 Δ*ponA*, *amyE*::P$_{hyperspank}$-*mNeonGreen-ponA*	This Study

[a] The *aph* and *cat* cassette are flanked by *frt* sites for removal by FLP recombinase. An *frt* scar remains following removal of the cassette using FLP expressed from pCP20.

[b] Strain constructions by P1 transduction are described using the shorthand: P1(donor) x recipient.

Table S3. Plasmids used in this study.

Plasmid	Genotype[a]	ori	Source/Reference
pKD13	*bla, aph* cassette flanked by *frt* sequence for recombineering	R6K	(Datsenko and Wanner, 2000)
pCP20	*cat bla cl857 P$_R$::FLP*	pSC101(*ts*)	(Datsenko and Wanner, 2000)
pHC739	attλ *cat lacI^q* P$_{tac}$::*sulA*	R6K	(Cho et al, 2014)
pCX16	*aadA sdiA*	pSC101	(Bendezu and de Boer, 2008)
pCS8	*attHK022 bla lacI^q* P$_{lac}$::*rodA*	R6K	(Sham et al, 2014)
pMM15	*attHK022 bla lacI^q* P$_{lac}$::*ponB*	R6K	This Study
pHC872	*attHK022 cat lacI^q* P$_{lac}$::*ponB*	R6K	This Study
pHC873	*attHK022 cat lacI^q* P$_{lac}$::*ponB(S247C)*	R6K	This Study
pHC878	*cat ponB(S247C)*	pSC101(*ts*)	This Study
pFB262	*bla lacI^q* P$_{lac}$::*mreB'-mCherry-'mreB*	ColE1	(Bendezu et al, 2009)
pHC892	*bla lacI^q* P$_{lac}$::*mreB'-mNeonGreen-'mreB*	ColE1	This Study
pHC897	attλ *cat lacI^q* P$_{lac}$::*mreB'-mNeonGreen-'mreB*	R6K	This Study
pHC929	*attHK022 bla lacI^q* P$_{tetA}$::*mreB'-mNeonGreen-'mreB*	R6K	This Study
pHC817	*cat* P$_{lac}$::*pbpA*	ColE1	(Cho et al, 2014)
pHC857	*cat* P$_{lac}$::*pbpA-rodA*	ColE1	(Cho et al, 2014)
pHC938	*cat* P$_{lac}$::*pbpA-rodA(D262N)*	ColE1	This Study
pHC933	*attHK022 tetAR lacI^q* P$_{lac}$::*sfgfp-rodA*	R6K	This Study
pHC942	*attHK022 tetAR lacI^q* P$_{lac}$::*msfgfp-ponB*	R6K	This Study
pHC943	*attHK022 tetAR lacI^q* P$_{lac}$::*msfgfp-pbpA*	R6K	This Study
pDHL940	pUC19-HaloTag H7-FRT-Kan[R]-FRT	pUC	(Ke et al., 2016)
pHC949	*attHK022 tetAR lacI^q* P$_{lac}$::*Halo-ponB*	R6K	This Study
pPR104	*attHK022 tetAR lacI^q* P$_{lac}$::*msfgfp-ponA*	R6K	This Study

[a] P$_R$, P$_{tac}$, P$_{lac}$, and P$_{tetA}$ indicate the phage λR, trp/lacUV5 hybrid, lac operon, and tetracycline resistance promoters, respectively.

Table S4. *B. subtilis* primer list

primer name	sequence (5'-3')
oMD191	TTTGGATGGATTCAGCCCGATTG
oMK138	TCTTTCGGTAAGTCCCGTCTAGCCTTGCCCTCACCCCAAAGGTGACGGCTTTTTTGT
oMK100	ATAACAATTAAGCTTTAAGGAGGAACTACCATGGTTTCGAAAGGAGAGGAGG
oMK087	AAAATTAACGTACTGATTGGGTAGTCTAGAATGGTTTCGAAAGGAGAGGAGGATAATATG
oMK086	ATGGTTTCGAAAGGAGAGGAGGATAATATGCAGGGAGCACTGGTCAACTACCG
oMK078	TGGCCTGAGCCCGGTCCCTGGCCAGATCCCTCGAGCTTATAGAGTTCATCCATACCCATC
oMK050	GAGTCATCAATTTGTTCGTATGTGGACC
oMK047	TCTAGACTACCCAATCAGTACGTT
oMK027	AACATCTCAACCTTTCGTTAATCAACC
oMK013	GTAGTTGACCAGTGCTCCCTGTAAAACACAAACAAACTCATCATC
oMK009	CTGGCCAGGGACCGGGCTCAGGCCAAGGAAGCGGCATGTCAGATCAATTTAACAGCCGTG
oMK006	CGTGTACAAGCAAAGCAGAATGAAC
oMK002	CTGAGCGAGGGAGCAGAACATCTCAACCTTTCGTTAATCAACC
oMK001	GCCTTATCCTTTCCTCCGCC
oMD232	ggtagttcctccttaAAGCTTAATTGTTATCCGCTCACAAT
oMD197	TCACATACTCGTTTCCAAACGGATC
oMD196	GGGCAAGGCTAGACGGG
oJM29	CAGGGAGCACTGGTCAAC
oJM28	TTCTGCTCCCTCGCTCAG

8

Supplemental Experimental Procedures

Media, bacterial strains, plasmids, and culture conditions for *E. coli* strains.
Cells were grown in LB (1% tryptone, 0.5% yeast extract, 0.5% NaCl) or minimal M9 medium supplemented with 0.2% casamino acids (CAA) and carbon source (0.4% glycerol or 0.2% glucose or maltose) as indicated. The bacterial strains and plasmids used in this study are listed in Tables S2 and S3, respectively, and a description of their construction or isolation in the genetic selection is given below.

Construction of *E. coli* strains with multiple deletions
E.coli strains with multiple deletion mutations were made by sequential introduction of each deletion from the Keio mutant collection [12] via P1 transduction followed by removal of the *aph* cassette using FLP expressed from pCP20, leaving a *frt* scar sequence at each deletion locus. Correct orientation of the DNA flanking *frt* sequences in multiple deletion mutants was confirmed for all the deletions in each mutant.

Construction of an MTSES-sensitive *E. coli* PBP1b variant
To test the effect of aPBP inhibition on cell wall synthesis and turnover, we sought a way to rapidly block the PGT activity of aPBPs. Moenomycin, a known inhibitor of the PGT activity of aPBPs, is not ideal for aPBP inhibition in WT *E.coli* because it cannot cross the outer membrane layer to access aPBPs. Instead, it was recently shown that a small cysteine-reactive molecule, MTSES [sodium (2-sulfonatoethyl)methanethiosulfonate], can be used in conjunction with a cysteine-substitution mutant to specifically block the activity of a surface exposed enzyme [13]. PBP1B was chosen for the development of a MTSES-blockable aPBP system because it is the major aPBP in *E.coli* and a structural information was also available for this protein [14]. Thirteen cysteine substitution variants of PBP1b were constructed with changes mapping within the moenomycin binding surface of PBP1B [14]. Alleles encoding each variant were cloned under control of the *lac* promoter in the CRIM plasmid pHC872 backbone (*attHK022*, P$_{lac}$::*ponB*) and the resulting plasmids were integrated into HC518 [⊗*ponA*::*frt* P$_{ara}$::*ponB*]. The functionality of each *ponB* allele was assessed by testing their ability to correct the PBP1a- PBP1b- synthetic lethality of HC518 grown on M9 glucose minimal medium supplemented with 100 µM IPTG.
Cysteine substitution mutants that were functional were further screened for the loss of activity upon MTSES treatment. This screen utilized the rapid lysis phenotype manifested in cells inhibited for aPBP activity in combination with 10 µg/mL cephalexin. Treatment of WT *E.coli* with 10 µg/mL cephalexin causes continued growth as cell filaments. However, lysis is observed in 20 min when aPBPs are also inhibited. We therefore screened the functional PBP1b cysteine substitution mutants for their response to treatment with 10 µg/mL cephalexin with or without 1mM MTSES using a VersaMax microplate reader (Molecular Devices). PBP1b(S247C) was identified as a variant that supports the growth similar to WT PBP1b but specifically leads to rapid lysis when cells producing the variant as the main aPBP are treated with 10 µg/mL cephalexin and 1mM MTSES.

Introducing *ponB(S247C)* mutation at the native *E. coli* locus

Allele exchange of *ponB(247C)* at the native locus was performed by using a temperature-sensitive plasmid pMAK700 as described [15]. Eighteen hundred bases of DNA flanking the *ponB(S247C)* mutation were PCR amplified from pHC873 using primers 5'-GCTA*ATCGAT*GAAAATCGGGCTTTTGCGCCTGAATATTGC-3' and 5'-GCTA*GCTAGC*AGATTTACCGTCGGCACGTTCATCG-3'. The resulting PCR product was digested with NheI and ClaI and ligated with pMAK700 digested with the same enzymes to generate pHC878. Plasmid integration and excision events at the *ponB* locus were selected utilizing the temperature-sensitive replication initiation of pHC878 to obtain strains with *ponB(S247C)* mutation at the native chromosomal locus.

Introduction of the *imp4213* allele

The *imp4213* allele was introduced into recipient strains by P1 transduction using its genetic linkage to *leu* marker. First, a *leu::Tn10* marker was introduced into the recipient strains by selecting for tetracycline resistance. Then, *imp4213* was introduced into the *leu* auxotrophs by P1 transduction followed by selection for leucine prototrophy on M9-glucose agar plates. For efficient P1 lysate preparation from an *imp4213* strain, a strain that has a suppressor mutation at the *bamA* locus in addition to *imp4213* (JAB027) was used. The resulting P1 transductants were screened for the sensitivity to 10 µg/mL erythromycin to identify isolates that acquired *imp4213* allele along with the WT *leu* locus.

Generation of *mreB* sandwich fusions at the native *E. coli mre* locus

Sandwich fluorescent protein fusions of *mreB* were introduced at the native locus using the recombineering strain CH138/pCX16, which harbors a defective lambda prophage as a temperature-inducible source of the recombination genes [16]. CH138/pCX16 is also deleted for native *galK* and has a *galK* cassette inserted in the middle of *mreB* (replacing the codon for G228). The strain is viable due to suppression of the Rod system defect by elevated FtsZ levels promoted by *sdiA* on pCX16. Fragments with one kb of sequence flanking *mNeonGreen* or *mCherry* in plasmid-borne *mreB*-fluorescent protein sandwich fusions were amplified with the primers 5'-AACGGTGTGGTTTACTCCTCTTCTGTG-3' and 5'-TTCCAGTGCAACCATTACCGCGCTCAC-3' using pFB262 or pHC892 as templates. After the recombineering with the resulting PCR products, cells that replaced *galK* with fluorescent protein fusions at the *mreB* locus were selected on M9 minimal agar containing 0.2% 2-deoxy-galactose, which is converted to toxic 2-deoxy-galactose-1-phosphate if cells remain GalK+.

Generation of *E. coli ΔrodA::aph*

A *rodA* deletion was constructed similar to deletions in the Keio collection [12] using a TB10(attHKCS8) recombineering strain that expresses *rodA* under control of the *lac* promoter. A PCR product for *ΔrodA::aph* construction was amplified using pKD13 [8] as a template with the primers 5'-

AAAATCCAGCGGTTGCCGCAGCGGAGGACCATTAATCATGATTCCGGGGATCCGT
CGACC-3' and 5'-
CTTACGCATTGCGCACCTCTTACACGCTTTTCGACAACATTGTAGGCTGGAGCTGC
TTCG-3' and recombineering was performed as described previously [17].

E. coli plasmid construction

pHC872 and pHC873
The *ponB* gene was amplified with primers 5'-
GTCA*TCTAGA*GAAAATCGGGCTTTTGCGCCTG-3' and 5'-
GTCA*CTCGAG*ATGGGATGTTATTTTACCGGATGGC-3'. The resulting fragment was
digested with XbaI and XhoI and ligated to pTB183 digested with XbaI and SalI to
generate pMM15. The *bla* antibiotic resistance cassette of pMM15 was replaced with a
cat cassette from pHC514 by replacing the NotI-XbaI fragment to generate pHC872.
The *ponB(S247C)* mutation was introduced in pHC872 using QuikChange mutagenesis
with the primer 5'-
CATGATGGAATCAGTCTCTAC<u>TGC</u>ATCGGACGTGCGGTGCTGGCA-3' to generate
pHC873.

pHC897
The *mCherry* sequence of pFB262 was replaced with *E.coli* codon-optimized
mNeonGreen (IDT synthesis) using XhoI and AscI to generate pHC892. The *mreB-*
^{SW}mNeon fragment of pHC892 was removed with XbaI and HindIII and cloned under
control of the *lac* promoter of a pHC514 derivative to generate pHC897.

pHC929
The *mreB-^{SW}mNeon* fragment was liberated from pHC892 by digestion with XbaI and
HindIII and *tetR*-P$_{tetA}$ (IDT synthesis) digested with BglI and XbaI were assembled in a
pTB183 derivative using BglII and HindIII to generate pHC929.

pHC938
pHC938 was generated by introducing the *rodA(D262N)* mutation into pHC857 using an
overlap extension mutagenesis protocol. *rodA(D262N)* was amplified using primers 5'-
AAATCC*GGTACC*GCTCAGGTC-3' and 5'-GTATCGGTGAT*AAGCTT*CTGC-3' and a
mutagenizing primer set 5'-CCGAACGCCATACT**A**ACTTTATCTTCGCGGTACTGG-3'
and 5'-GCGAAGATAAAG<u>TT</u>AGTATGGCGTTCGGGGAGAAATTC-3'. The mutated
base is indicated in bold. The resulting PCR product for *rodA(D262N)* was digested with
KpnI and HindIII and ligated to pHC857 digested with the same enzymes to generate
pHC938.

pHC933
The *sfgfp* fragment was liberated from pTB230 with XbaI and BamHI digestion and *rodA*
amplified with 5'-

GTCA*GGATCC*GAGGCCATTACGGCCATGACGGATAATCCGAATAAAAAAACATTCT
GGG-3' and 5'-GTCA*GTCGAC*TTATTATTGGCCGAGGCGGCCTTACACGCTTTTC-3'
and digested with BamHI and SalI. The fragments were assembled in pNP20 using XbaI
and SalI to generate pHC933.

pHC942, pHC943, and pPR104
E.coli codon-optimized *msfgfp* (IDT synthesis) digested with XbaI and BamHI, and the
ponB sequence amplified with 5'-GTAC*GGATCC*CCGCGCAAAGGTAAGGG-3' and 5'-
GTCA*CTCGAG*ATGGGATGTTATTTTACCGGATGGC-3' and digested with BamHI and
XhoI were assembled in pNP20 by using XbaI and SalI to generate pHC942. The *ponB*
of pHC942 was then replaced with *pbpA* sequence amplified with 5'-
GCTA*GGATCC*AAACTACAGAACTCTTTTCGCGACTATACG-3' and 5'-
CTTCACGTTCGCTCGCGTATCGGTG-3' using BamHI and HindIII to generate
pHC943. pPR104 was constructed by replacing *ponB* of pHC942 with *ponA* sequence
amplified with 5'-GCTA*GGATCC*AAGTTCGTAAAGTATTTTTTGATCC-3' and 5'-
GCTA*AAGCTT*AGAACAATTCCTGTGCCTCGCCAT-3' using BamHI and HindIII.

pHC949
HaloTag sequence was amplified by using pDHL940 as a template with 5'-
GCTA*TCTAGA*TT<u>TAAGAAGG</u>AGATATACATATGGCAGAAATCGGTACTGGCTTTCC
ATTC-3' and 5'-GCTA*GGATCC*GGAAATCTCCAGAGTAGACAGC-3'. The resulting
PCR product was digested with XbaI and BamHI, and ligated to pHC942 digested with
the same enzymes to replace *msfgfp* sequence with *HaloTag* sequence.

Measurement of PG synthesis and turnover
The effect of blocking aPBP activity with MTSES on PG synthesis and turnover in beta-
lactam-treated *E.coli* cells was examined essentially as described previously [7].
HC533(attλHC739), a *ΔlysA ΔampD* strain which expresses PBP1b(S247C) as a sole
aPBP, was grown overnight in M9-glycerol medium supplemented with 0.2% casamino
acids. The overnight culture was diluted to an OD_{600} = 0.04 in the same medium and
grown to an OD_{600} between 0.26 - 0.3. Then, divisome formation was blocked by
inducing *sulA* expression for 30 min from a chromosomally integrated P_{tac}::*sulA*
construct (pHC739) by adding IPTG to 1 mM. After adjusting the culture OD_{600} to 0.3,
MTSES (1mM), A22 (10 µg/mL), mecillinam (10 µg/mL), and/or cefsulodin (100 µg/mL)
were added to the final concentrations indicated and cells were incubated for 5 min.
Following drug treatment, 1 µCi of [³H]-meso-2,6-Diaminopimelic acid (mDAP) was
added to 1mL of each drug-treated culture and incubated for 10 min to label the newly
synthesized PG and its turnover products. After the labeling, cells were pelleted,
resuspended in 0.7 ml water, and heated at 90°C for 30 min to extract water-soluble
compounds. After the hot water extraction, insoluble material was pelleted by
ultracentrifugation (200,000 x g for 20 min at 4°C). The resulting supernatant was then
removed, lyophilized, and resuspended in 0.1% formic acid for HPLC analysis and
quantification of turnover products as described previously [7]. To determine [³H]-mDAP
incorporated into the PG matrix, the pellet fraction was washed with 0.7 mL buffer A (20
mM Tris-HCl, pH 7.4, 25 mM NaCl) and resuspended in 0.5 mL buffer A containing 0.25

mg lysozyme. The suspensions were incubated overnight at 37°C. Insoluble material was then pelleted by centrifugation (21,000 x g for 30 min at 4°C), and the resulting supernatant was mixed with 10 mL EcoLite (MP biomedicals) scintillation fluid and quantified in Microbeta Trilux 1450 liquid scintillation counter (Perkin-Elmer).

Quantification of MTSES labeling of PBP1b(S247C)

To quantify the efficiency of MTSES binding to PBP1b(S247C) under experimental growth conditions, a culture of HC533(attλHC739) (100 mL) was grown to $OD_{600} = 0.3$ in M9-glycerol medium supplemented with 0.2 % casamino acids at 30°C with *sulA* induction for 30 minutes. Then, the culture was split into two 50 mL portions and treated with either 1mM MTSES or DMSO for 5 min. Immediately after MTSES/DMSO treatment, cultures were cooled on ice and cells pelleted at 4,000 x g for 5 min at 4°C. The cell pellets were washed once with 1X ice-cold PBS, resuspended in 500 µL 1X PBS containing 10 mM EDTA and 20 mM 2-iodoacetamide, and incubated for 20 min at room temperature to alkylate the cysteine residues not modified by MTSES. After the 20 min incubation, 20kU of Ready-lyse lysozyme (Epicentre) was added to each cell suspension and incubation was continued for a further 10 min at room temperature. Cells were disrupted by sonication and membrane fractions were pelleted by ultracentrifugation at 200,000 X g for 20 min at 4°C. The membrane fractions were then washed with 1X PBS once and resuspended in 1 mL immunoprecipitation (IP) buffer (100mM Tris, pH7.4, 300mM NaCl, 2% Triton X-100). Ten microliters of anti-PBP1b antiserum was added to the resuspension and the resuspension was incubated overnight in the cold room with gentle agitation. The samples were then mixed with 50 µL of IP buffer-equilibrated protein A/G magnetic beads (Millipore) and incubated for further 4 hrs in the cold room with gentle agitation. Then, the beads were washed three times with IP buffer and then three times with a buffer containing 100mM Tris, pH7.4 and 300mM NaCl.

Proteins bound on the beads were fragmented by on-bead digestion with 0.1µg trypsin (#V511C, Promega) in 300µl buffer (20mM Tris-HCl, pH8, 150mM NaCl) overnight at 37°C with gentle agitation. After digestion, peptide samples were acidified with 10% TFA to a pH between 1-2, desalted using a 96-well plate embedded with C18 resin (Thermo Scientific) and dried by vacuum centrifugation. Samples were resolubilized in 20 µl of 0.1% TFA and 5 µl of each sample was analyzed by nanoLC-MS/MS [18] with a HPLC gradient (NanoAcquity UPLC system, Waters; 5%–35% B in 110min; A=0.1% formic acid in water, B=0.1% formic acid in acetonitrile). Peptides were resolved on a self-packed analytical column (50cm Monitor C18, Column Engineering) and introduced to the mass spectrometer (Q Exactive HF) at a flow rate of 30 nl/min (ESI spray voltage=3.5kV). The mass spectrometer was programmed to operate in data dependent mode such that the ten most abundant precursors in each full MS scan (resolution=120K; target=5e5; maximum injection time=500ms; scan range= 300 to 2,000 m/z) were subjected to HCD (resolution=15K; target=5e4; maximum injection time=200ms; isolation window=1.6m/z; NCE=27, 30; dynamic exclusion=15seconds). MS/MS spectra were matched to peptide sequences using Mascot (version 2.2.1) after

conversion of raw data to .mgf using multiplierz scripts [19]. Search parameters specified trypsin digestion with up to two missed cleavages, as well as variable oxidation of methionine and carbamidomethylation of cysteine residues. Precursor and product ion tolerances were 10 ppm and 25 mmu, respectively. Targeted scan experiments were performed in a similar fashion while dynamic exclusion was disabled and inclusion was enabled for the following peptides: HFYEHDGISLYCIGR (carbamidomethyl cysteine: z=4, m/z=467.4703; z=3, m/z=622.9579; z=2, m/z=933.9332), HFYEHDGISLYCIGR (MTSES-cysteine: z=4, m/z=488.2050; z=3, m/z=650.6042; z=2, m/z=975.4026), VWQLPAAVYGR (z=2, m/z=630.3484), LLEATQYR (z=2, m/z=497.2718), QFGFFR (z=2, m/z=401.2058), DSDGVAGWIK (z=2, m/z=524.2589). Peak area integration was carried out using the Thermo Xcalibur Qual Browser (version 3.0.63, Thermo Fisher Scientific).

Bocillin-binding assays
Cultures of HC545, HC596(attHKHC943), and HC576(attHKHC942) were grown overnight at 37°C in M9-glucose medium supplemented with 0.2% casamino acids, with induction of *msfgfp-pbpA* or *msfgfp-ponB* with 25 μM IPTG. Cells in the overnight cultures were washed to remove IPTG and diluted to an OD_{600} = 0.001 in 15 ml of M9-glucose medium supplemented with 0.2% casamino acids and the indicated concentrations of IPTG. The cultures were then incubated at 37°C until the OD_{600} reached 0.4 to 0.5. A subset of cultures were treated with 10 μg/mL mecillinam (specific for PBP2) or 100 μg/mL cefsulodin (specific for PBP1b) for 5 min prior to harvesting. Cells were then harvested by centrifugation at 4°C, washed with ice-cold 1X phosphate-buffered saline (PBS) twice, resuspended in 500 μL 1X PBS containing 10 mM EDTA and 15 μM Bocillin (Invitrogen), and incubated at room temperature for 15 min. After the incubation, the cell suspensions were washed with 1X PBS once, resuspended in 500 μL 1X PBS, and disrupted by sonication. After a brief spin for 1 min at 4,000 X g to remove undisrupted cells, membrane fractions were pelleted by ultracentrifugation at 200,000 X g for 20 min at 4°C. The membrane fractions were then washed with 1X PBS and resuspended in 50 μL 1X PBS. Resuspended samples were mixed with 50 μL 2X Laemmli sample buffer and boiled for 10 min at 95°C. After measuring the total protein concentrations of each sample with NI-protein assay (G-Biosciences), 25 μg of total protein for each sample was then separated on a 10% SDS-PAGE gels and the labeled proteins were visualized using a Typhoon 9500 fluorescence imager (GE Healthcare) with excitation at 488 nm and emission at 530 nm.

Bocillin-binding assays for *Bacillus subtilis* strains were performed basically in the same way as in *E.coli* strains. Overnight cultures grown in CH medium at room temperature were diluted to OD_{600} = 0.04 - 0.07 in 5 mL fresh CH medium containing the indicated concentrations of IPTG and incubated at 37°C. When the cultures reached exponential phase, cells were pelleted, washed with ice-cold 1X PBS, and resuspended with 100 μL 1X PBS containing 15 μM Bocillin (Invitrogen), and incubated for 15 min at room temperature. Then, cells were washed in 1X PBS, resuspended 0.5 mL 1X PBS containing 20kU Ready-lyse lysozyme (Epicentre), and incubated for 15 min at room

temperature. The cells were disrupted by sonication and the membrane fraction was isolated by ultracentrifugation. A total of 16 µg of protein for each sample was separated on a 10% SDS-PAGE gels and visualized as described above for *E. coli*.

Microscopy of *E. coli* cells

Overnight cultures with strain-specific inducer levels were diluted in fresh culture medium and grown for at least 3 hours at 37 °C to an OD_{600} below 0.6. Cells were concentrated by centrifugation at 7,200 x *g* for 3 min and applied to No. 1.5 cover glass under 5 % agarose pads with culture medium, except for microscopy with MTSES, which was performed using the CellASIC ONIX microfluidic platform from EMD Millipore.

For msfGFP-PBP2 tracking, M9-glucose-CAA medium was used with 25 µM IPTG. For sfGFP-RodA tracking, M9-maltose-CAA medium was used with 80 µM IPTG. For msfGFP-PBP1b imaging, M9-glucose-CAA medium was used with a beginning concentration of 20 µM IPTG, diluted to 13 µM final IPTG before expansion at 37 °C. For MreB-^{SW}Neon tracking with MTSES treated cells, M9-glucose-CAA medium was used with 100 µM IPTG.

For MreB-^{SW}Neon tracking following RodA(WT) or RodA(D262N) overproduction, M9-maltose-CAA medium was used with the addition of 0.8 ng/µL anhydrotetracycline before growth at 37 °C. For experiments following the effect of RodA variant production after 210 min induction, cells were first grown in liquid culture for 120 min under inducing conditions (1mM IPTG) before concentration and imaging. IPTG (1 mM) was included in the agarose pads used for imaging.

Microscopy of *B. subtilis* cells

Overnight cultures grown in CH medium were diluted in fresh medium and grown for at least 3 hours at 37 °C to an OD_{600} below 0.3. Cells were concentrated by centrifugation at 6000 x *g* for 30 seconds and applied to No. 1.5 cover glass under 2 % agarose pads with CH medium. For PBP1 imaging, no inducer was added to the cultures; leaky expression of mNeonGreen-PBP1 was sufficient for particle tracking experiments. All cells were imaged at 37 °C under an agar pad with the top surface exposed to air.

For measurements of growth rate, overnight cultures grown in LB medium were diluted in fresh medium and grown for at least 3 hours at 37 °C and to an OD_{600} below 0.3. The culture was diluted to an OD_{600} of 0.07, and its growth curve was measured in a Growth Curves USA Bioscreen-C Automated Growth Curve Analysis System.

For measurements of cell widths, overnight cultures grown in CH medium were diluted in fresh medium (with addition of 10 μM IPTG where indicated) for at least 3 hours at 37 °C and to an OD_{600} below 0.3. Cells were stained with FM 5-95 (ThermoFisher Scientific) and imaged under agarose pads as described above.

Particle Tracking Microscopy

Total internal reflection fluorescence microscopy (TIRF-M) and phase contrast microscopy were performed using a Nikon Eclipse Ti equipped with a Nikon Plan Apo λ 100X 1.45 objective and a Hamamatsu ORCA-Flash4.0 V2 (C11440-22CU) sCMOS camera. Except where specified, fluorescence time-lapse images were collected by continuous acquisition with 1,000 ms exposures. Microscopy was performed in a chamber heated to 37 °C.

Widefield Epifluorescence Microscopy
Widefield epifluorescence microscopy was performed on the instrument described above, and for some samples, on a DeltaVision Elite Microscope equipped with an Olympus 60x Plan Apo 60x 1.42 NA objective and a PCO.edge sCMOS camera. Cell contours and dimensions were calculated using the Morphometrics software package [20].

Particle tracking
Particle tracking was performed using the software package FIJI [21,22] and the TrackMate plugin. For calculation of particle velocity, the scaling exponent α, and track orientations relative to the midline of the cell, only tracks persisting for 7 frames or longer were used. Particle velocity for each track was calculated from nonlinear least squares fitting using the equation $MSD(t) = 4Dt + (vt)^2$,
where MSD is mean squared displacement, t is time interval, D is the diffusion coefficient, and v is speed. The maximum time interval used was 80 % of the track length. Tracks were excluded from further evaluation if the contribution of directional motion to the MSD was less than 0.01 nm/s. Tracks were also excluded if R^2 for log MSD versus log t was less than 0.9, indicating a poor ability to fit the MSD curve. For PBP2, R^2 and speed filtering together resulted in the exclusion of ~50 % of detected tracks. Track overlays in figures include all tracks 7 frames or longer to illustrate the performance of the track detection algorithms.

Track angles relative to the cell axis were taken to be the direction of the line produced by orthogonal least squares regression using all of the points in each track; cell axis angles were determined by finding cell outlines and axes using the Morphometrics software package [20].

Analysis of PBP1 diffusion. Tracking of *B. subtilis* mNeon-PBP1 in strains MK210 and MK287 was performed using the u-track 2.0 software package [23]. Resulting trajectories were then manually filtered to minimize particle detection and linking errors. The frame-to-frame vector displacements along these trajectories were then calculated. The magnitude of each of the displacements was taken, and the cumulative distribution function (CDF) of the pool of displacements across all movies in a condition was calculated. The CDF of the displacement magnitudes was then fit to an analytical function describing a diffusion process whereby one or more unique states of diffusion were occurring. The analytical form of the two-state model used in the results is:

$$P(r, \Delta t) = 1 - we^{-\left(\frac{r^2}{4D_1\Delta t}\right)} - (1-w)e^{-\left(\frac{r^2}{4D_2\Delta t}\right)}$$

where $P(r, \Delta t)$ is the cumulative probability of a displacement of magnitude r given the observation period Δt, diffusion coefficients D_1, D_2, and the relative fractions between those two states w. For a simpler, one-state model, $w = 1$.

The fitting was performed in MATLAB using a nonlinear least-squares algorithm with 500 restarts to the initial parameters so as to find a close approximation to the true parameters of the model. Residuals of the model fit were calculated and used in the determination of the number of distinct diffusive species present within the dataset.

B. subtilis strain construction

For MK005 [Δ*ponA*] construction, the homology region upstream of *ponA* was amplified from Py79 DNA using oligos oMK001 and oMK002. The *cat* cassette was amplified from pGL79 using oligos oJM28 and oJM29. The homology region downstream of *ponA* was amplified from Py79 DNA using oligos oMK006 and oMK013. The three fragments were fused using isothermal assembly [24] and transformed into Py79 to give MK005 by selecting on chloramphenicol agar.

For MK095, a native functional fusion of mNeonGreen to PBP1 was constructed by isothermal assembly [24] and was recombined into the chromosome of Py79 using counterselection to produce a marker-less strain without any remaining scars. The homology region upstream of *ponA*, fused to the first 30 bases of the coding sequence of mNeonGreen, was amplified from Py79 DNA using oMK001 and oMK027. The *cat* cassette, the P_{xyl} promoter sequence, and the *mazF* coding sequence were amplified as a fused fragment from template DNA using primers oMK047 and oMK086. The coding sequence of mNeonGreen was amplified from a gBlock using primers oMK078 and oMK087. The downstream homology region encoding a portion of the PBP1 (*ponA*) coding sequence was amplified from Py79 DNA using oMK009 and oMK050. These fragments were fused using isothermal assembly and transformed into Py79 to give MK093 upon selection for chloramphenicol resistance. Since the primers oMK078 and oMK009 contained the sequence for a 15-amino acid flexible linker, the fused product encoded an mNeonGreen-PBP1 fusion protein. The presence of a fragment of the mNeonGreen coding region upstream of *cat* provided a direct repeat to allow for spontaneous removal of the *cat-mazF* sequence by recombination. MK093 was grown in LB medium for 4 hours to allow time for recombination, and 200 μl cells were plated on a LB plate containing 30 mM xylose. This selected for cells in which removed the *cat-mazF*, yielding a scar-less functional fusion protein under the control of the native PBP1 promoter.

Strains MK210 and MK287 encoding an inducible version of the mNeonGreen-PBP1 fusion protein were constructed by isothermal assembly. The homology region upstream of *amyE*, the *erm* cassette, and the *LacI*-$P_{hyperspank}$ promoter construct were amplified as a fused fragment from template DNA using primers oMD191 and oMD232. The mNeonGreen-PBP1 coding sequence was amplified from MK095 DNA using primers oMK100 and oMK138. The homology region downstream of *amyE* was amplified from

17

Py79 DNA using oMD196 and oMD197. The fragments were fused using isothermal assembly and transformed into Py79 to give MK210. Genomic DNA from MK005 (Δ*ponA*::cat) was transformed into MK210 to give MK287, a strain in which the mNeonGreen-PBP1 fusion protein was the only copy of PBP1.

References

1.   Paintdakhi, A. *et al.* Oufti: an integrated software package for high-accuracy, high-throughput quantitative microscopy analysis. *Molecular Microbiology* **99,** 767–777 (2015).

2.   Grimm, J. B. *et al.* A general method to improve fluorophores for live-cell and single-molecule microscopy. *Nat Methods* **12,** 244–250 (2015).

3.   Guyer, M. S., Reed, R. R., Steitz, J. A. & Low, K. B. Identification of a sex-factor-affinity site in E. coli as gamma delta. *Cold Spring Harb Symp Quant Biol* **45 Pt 1,** 135–140 (1981).

4.   Johnson, J. E., Lackner, L. L., Hale, C. A. & de Boer, P. A. J. ZipA is required for targeting of DMinC/DicB, but not DMinC/MinD, complexes to septal ring assemblies in Escherichia coli. *J. Bacteriol.* **186,** 2418–2429 (2004).

5.   Paradis-Bleau, C. *et al.* Lipoprotein cofactors located in the outer membrane activate bacterial cell wall polymerases. *Cell* **143,** 1110–1120 (2010).

6.   Bernhardt, T. G. & de Boer, P. A. J. Screening for synthetic lethal mutants in Escherichia coli and identification of EnvC (YibP) as a periplasmic septal ring factor with murein hydrolase activity. *Molecular Microbiology* **52,** 1255–1269 (2004).

7.   Cho, H., Uehara, T. & Bernhardt, T. G. Beta-lactam antibiotics induce a lethal malfunctioning of the bacterial cell wall synthesis machinery. *Cell* **159,** 1300–1311 (2014).

8.   Datsenko, K. A. & Wanner, B. L. One-step inactivation of chromosomal genes in Escherichia coli K-12 using PCR products. *Proc Natl Acad Sci USA* **97,** 6640–6645 (2000).

9.   Bendezú, F. O. & de Boer, P. A. J. Conditional lethality, division defects, membrane involution, and endocytosis in mre and mrd shape mutants of Escherichia coli. *J. Bacteriol.* **190,** 1792–1811 (2008).

10. Bendezú, F. O., Hale, C. A., Bernhardt, T. G. & de Boer, P. A. J. RodZ (YfgA) is required for proper assembly of the MreB actin cytoskeleton and cell shape in E. coli. *EMBO J* **28,** 193–204 (2009).

11. Ke, N., Landgraf, D., Paulsson, J. & Berkmen, M. Visualization of Periplasmic and Cytoplasmic Proteins with a Self-Labeling Protein Tag. *J. Bacteriol.* **198,** 1035–1043 (2016).

12. Baba, T. *et al.* Construction of Escherichia coli K-12 in-frame, single-gene knockout mutants: the Keio collection. *Mol Syst Biol* **2,** 2006.0008 (2006).

13. Sham, L.-T. *et al.* Bacterial cell wall. MurJ is the flippase of lipid-linked precursors for peptidoglycan biogenesis. *Science* **345,** 220–222 (2014).

14. Sung, M.-T. *et al.* Crystal structure of the membrane-bound bifunctional transglycosylase PBP1b from Escherichia coli. *Proc Natl Acad Sci USA* **106,** 8824–8829 (2009).

15. Cho, H., McManus, H. R., Dove, S. L. & Bernhardt, T. G. Nucleoid occlusion factor SlmA is a DNA-activated FtsZ polymerization antagonist. *Proc Natl Acad Sci USA* **108,** 3773–3778 (2011).

16. Warming, S., Costantino, N., Court, D. L., Jenkins, N. A. & Copeland, N. G. Simple and highly efficient BAC recombineering using galK selection. *Nucleic Acids Res* **33,** e36–e36 (2005).

17. Yu, D. *et al.* An efficient recombination system for chromosome engineering in Escherichia coli. *Proc Natl Acad Sci USA* **97,** 5978–5983 (2000).

18. Ficarro, S. B. *et al.* Improved electrospray ionization efficiency compensates for diminished chromatographic resolution and enables proteomics analysis of tyrosine signaling in embryonic stem cells. *Anal. Chem.* **81,** 3440–3447 (2009).

19. Askenazi, M., Parikh, J. R. & Marto, J. A. mzAPI: a new strategy for efficiently sharing mass spectrometry data. *Nat Methods* **6,** 240–241 (2009).

20. Ursell, T. S. *et al.* Rod-like bacterial shape is maintained by feedback between cell curvature and cytoskeletal localization. *Proc Natl Acad Sci USA* **111,** E1025–34 (2014).

21. Schindelin, J. *et al.* Fiji: an open-source platform for biological-image analysis. *Nat Methods* **9,** 676–682 (2012).

22. Schneider, C. A., Rasband, W. S. & Eliceiri, K. W. NIH Image to ImageJ: 25 years of image analysis. *Nat Methods* **9,** 671–675 (2012).

23. Jaqaman, K. *et al.* Robust single-particle tracking in live-cell time-lapse sequences. - PubMed - NCBI. *Nat Methods* **5,** 695–702 (2008).

24. Gibson, D. G. *et al.* Enzymatic assembly of DNA molecules up to several hundred kilobases. *Nat Methods* **6,** 343–345 (2009).